Theoretical and experimental analysis of a thin elastic cylindrical tube acting as a non-Hookean spring

Antonio Šiber[1,*] and Hrvoje Buljan[2]
[1]*Institute of Physics, Bijenička cesta 46, 10000 Zagreb, Croatia*
[2]*Department of Physics, University of Zagreb, Bijenička cesta 32, 10000 Zagreb, Croatia*
(Received 13 October 2010; published 13 June 2011)

We analyze the (large) deformation and energy of a thin elastic cylindrical tube compressed between two plates parallel to the tube axis. The deformation is studied theoretically using a numerical calculation and the variational approach. The results are used to interpret the experimental data obtained by pressing tubes made from plastic-foil transparencies. We obtain a universal scaling relation that characterizes the response of the tube. Our results may serve as a benchmark for the application of variational methods to thin-walled nanoscale systems in order to obtain functional relations between the energy and the deformation.

DOI: 10.1103/PhysRevE.83.067601 PACS number(s): 46.70.De, 62.20.D−, 01.50.My

Large deformations of elastic bodies are typical in cases where tight packing is necessary due to particular constraints [1] or external pressure [2,3]. In many cases the systems of interest are nanoscale, e.g., DNA molecules in bacteriophage capsids [4], empty virus shells under osmotic pressure [3], and crystals of deformable, soft particles [5] such as fullerenes and carbon nanotubes [6]. There are also systems on a micronlength scale characterized by tight packing and pronounced deformation, such as epithelial tissues [7]. The elasticity of the systems of interest is often studied in the linear elasticity regime (see, e.g., Ref. [8]) where the characteristic deformations are small. However, to properly account for energies of tightly packed and/or constrained and strongly deformed structures, one needs to consider the elastic energies in the nonlinear regime. Yet the functional relations between force (energy) and deformation are derived mostly in the small-deformation regime [9]. Although strongly deformed bodies may be studied numerically using different variants of the finite element technique, functional relations that transparently relate energy and deformation are certainly of special use. Such analytical expressions are of importance in many applications, especially in nanoscale physics and cellular biophysics [7].

In this Brief Report we introduce a spring made by rolling a piece of thin elastic sheet to form a cylindrical tube. We predict small and large deformations of such a spring situated in between two parallel plates by using an approximate but completely adequate variant of the theory of elasticity. Our work presents a way to obtain reliable analytical approximations for strongly deformed systems using a variational approach. Although variational approaches are very convenient when examining strongly deformed systems, their validity and usefulness is not obvious. In particular, it is of interest to see whether simple trial functions for the shape of the deformed system yield a correct functional dependence of energy on the deformation variable (generalized extension). For the simple system that we have chosen for this study, we derive an analytical expression for the energy in the strongly deformed regime. To check the validity of the approach presented, we perform numerical calculations and determine a universal response curve of thin-walled tubes of different dimensions and elastic properties. We actually built the system of interest so as to provide reliable experimental data. The experimental data confirm the universal scaling curve that we obtained numerically through almost four orders of magnitude of the force.

The system that we have chosen is meant to model cases of large deformations in materials that are made of thin sheets. This is motivated by thin-sheet structures such as carbon nanotubes, fullerenes, and other similar structures made of graphene sheets [10,11], cellular membranes and vesicles [7,12] (made of a lipid bilayer), and protein shells (made of protein sheets), such as virus capsids [3,13,14] and microtubules [15]. One may wonder whether our (macroscopic) experimental setup and the classical theory of elasticity can be used as a model and an approach relevant for nanoscale systems. It has been shown that the energies of nanoscale thin-shelled systems (larger than about 2 nm [11]) can be very accurately determined using the theory of elasticity [10,11] (see also Ref. [16]), thus our work directly reflects on the systems of present interest.

The tube is pressed between two parallel plates as depicted in Fig. 1. The length of the parallel plates is larger than the length of the tube h, which makes the problem effectively one dimensional. As the tube deforms inextensionally, the stretching of the sheet can be neglected [17] and the elastic energy of the pressed tube is $E_{\mathrm{el}} = \kappa \int_S K^2 dS/2$, where κ is the bending (or flexural) rigidity of the sheet and $K = R_1^{-1} + R_2^{-1}$, where R_1 and R_2 are the principal radii of curvature at some point. We have implicitly assumed that both radii are much larger than the thickness of the sheet d. If the material the sheet is made of is isotropic, the bending rigidity κ is related to the Young modulus and Poisson ratio ν of the material as [17]

$$\kappa = \frac{Ed^3}{12(1-\nu^2)}. \tag{1}$$

Since the sheet is bent only along one direction, we can write the elastic energy in terms of the one-dimensional integral $E_{\mathrm{el}} = \kappa h \int_{\mathcal{C}} K^2 dl/2$, where $\mathcal{C}$ is the curve outlining the shape of the cylinder base and dl is the infinitesimal arc element

*asiber@ifs.hr

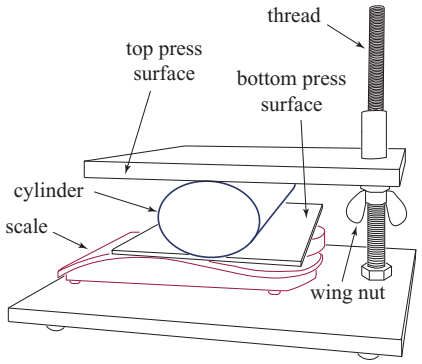

FIG. 1. (Color online) Illustration of the experimental setup.

of the curve $\mathcal{C}$ ($dS = h\,dl$). The force exerted by the pressed cylinder onto the plates can be measured by using a simple scale located below the bottom plate (see Fig. 1). It is useful to recognize that the effective mass m_e measured by the scale can be thought of as a mass that presses the spring from above due to gravity (the mass of the spring being neglected here). With this picture in mind, the total energy of the system is

$$\mathcal{E} = E_p + E_{\rm el} = 2m_e g b + \frac{\kappa h}{2}\int_{\mathcal{C}} K^2 dl, \qquad (2)$$

where $2b$ is the separation between the plates. For a given mass m_e, there is an equilibrium value of b at which $\partial\mathcal{E}/\partial b = 0$. The difficult part of the problem is to find the curve $\mathcal{C}$ that minimizes the elastic energy $E_{\rm el}$ for a given separation between the plates $2b$; the minimization should be performed with two constraints: The length of the curve is fixed (the sheet is inextensible) and the height of the object depicted by $\mathcal{C}$ is $2b$.

To explore the energetics of the problem analytically, we use two qualitatively different Ritz trial solutions (*Ansätze*) for curve $\mathcal{C}$: (i) the stadium-shaped curve made of two identical semicircles connected by two straight lines that touch the press plates (this profile is expected to be a good model for sufficiently large pressing forces and is often used for vesicles and cells in contact; see, e.g., Ref. [7]) and (ii) an ellipse (expected for small forces) that touches each plate at one point.

The energy of the stadium profile is calculated as follows. Flat pieces of the profile contribute nothing to the elastic energy since there $K = 0$; the curved parts are two halves of a cylinder of height h and radius b, where $K = b^{-1}$, so that we have

$$\mathcal{E} = 2m_e g b + \frac{\pi\kappa h}{b}. \qquad (3)$$

The spring will be in equilibrium when $d\mathcal{E}/db = 0$, i.e., when

$$b = \sqrt{\frac{\kappa\pi h}{2m_e g}}. \qquad (4)$$

This solution is expected to be correct only for sufficiently large loads. Note that the stadium profile fulfills the inextensionality requirement when $b < b_0$.

The elastic energy when $\mathcal{C}$ is an ellipse with a circumference equal to $2\pi b_0$ (this is the inextensionality requirement; b_0 is the radius of the cylinder in its unladen state) can be expressed in terms of elliptic integrals. However, since this *Ansatz* makes sense only for small deformations where the major and minor

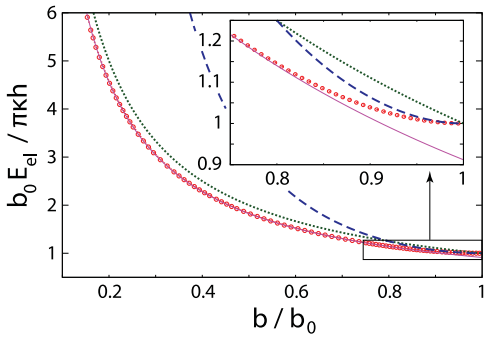

FIG. 2. (Color online) Theoretical predictions for the spring energies. The circles show the numerical results, the dotted line is the prediction of the variational method based on the stadium profile, and the dashed line corresponds to the elliptic profile. The solid line shows the stadium profile energy multiplied by 0.912.

axes of the ellipse, a and b, are close, these integrals can be Taylor expanded to yield

$$\lim_{a\to b} E_{\rm el} = \frac{\pi h\kappa}{b}\left(\frac{5(b_0/b) - 4\,(b_0/b)^2 - 2}{3 - 4(b_0/b)}\right). \qquad (5)$$

The energy [Eq. (5)] differs from the elastic energy of the stadium profile by the multiplicative factor in large parentheses, which is smaller than one in the interval $b \in [0.80b_0, b_0]$, where the elliptic profile is the better *Ansatz*. From Eq. (5) we derive the spring equilibrium for small deformations: $b = b_0 - m_e g b_0^3/7\pi h\kappa$ (only first-order terms are kept).

The curve $\mathcal{C}$ that minimizes the elastic energy for a given separation between the press plates can be found numerically. To this end we discretize the profile of the deformed spring in N points and reformulate the elastic energy functional to depend on coordinates of these points. The functional is minimized using a particular variant of the conjugate gradient minimization (see, e.g., Refs. [3,11,14]). The constraints of the inextensibility of the sheet and the impenetrability of the top and bottom press surfaces are implemented through energy penalty for all configurations that violate the constraints.

In Fig. 2 we show the theoretical predictions for the spring energy. The circles show the numerically obtained energies, the dotted line is the prediction based on the stadium profile, and the dashed line is the prediction based on the elliptical profile. We see that the calculation for the stadium profile quite nicely follows the trend of the numerical results in the range $b/b_0 > 0.7$. In fact, multiplying the stadium results by a factor 0.912 gives a solid line that fits the numerical data to a precision better than 0.8% in the range $0.15 < b/b_0 < 0.7$, clearly vindicating the utility of the stadium *Ansatz* and the analytical trend that it predicts. The energies based on the elliptical profile are, as expected, accurate only when $b \approx b_0$.

The solution of the problem can be scaled so that it becomes universal. This means that appropriately scaled measurements, irrespective of the spring properties (equilibrium radii b_0, heights h, and bending rigidities κ), should all fall on the universal curve. Such a scaled solution depends only on an adimensional parametrization: The adimensional parameter that uniquely determines the spring shape is b/b_0 and an

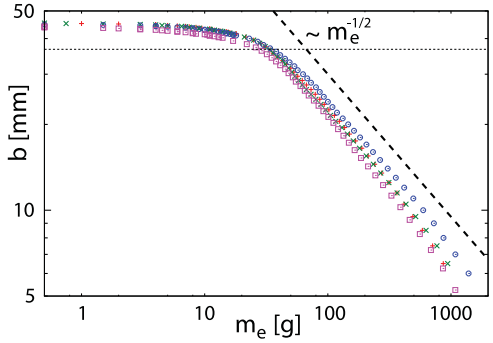

FIG. 3. (Color online) Half of the separation between the plates b vs scale reading m_e for four springs made from identical foils. The dashed line shows the slope expected for the $b \propto m_e^{-1/2}$ dependence. The thin dotted line shows $b = 0.7\langle b_0 \rangle$. See text for details.

appropriate scale of elastic energy is $\pi\kappa h/b_0$. The energy-shape dependence can thus be written as

$$\frac{b_0}{\pi\kappa h} E_{\rm el} = \mathcal{U}\left(\frac{b}{b_0}\right) \equiv \bar{E}_{\rm el}, \tag{6}$$

where $\mathcal{U}(b/b_0)$ is the universal function characteristic for our problem. The appropriately scaled energy (adimensional) is denoted by an overline ($\bar{E}_{\rm el}$), as all the adimensional quantities will be in the following.

The tubes that were used in our experiments are constructed from thin transparent foils (made of polymer material), which are usually used for plastic covers for strip and spiral book binding. Their size is that of A4 paper, $W = 210$ mm and $L = 297$ mm. The tube is made by rolling a foil in a cylinder, either along its width W or its length L ($L > W$), and by using the adhesive tape to fix the cylinder. For accurate measurements, the width of the overlapping region where the adhesive tape is applied should be as small as possible ($\sim$2 mm in our measurements). The response of the spring is measured in a press with two parallel plates as illustrated in Fig. 1. The upper plate is driven by a wing nut with a known pitch that enables one to precisely determine the shift of the top plate. An ordinary kitchen scale located below the lower plate measures the force that the tube exerts on the plates.

In Fig. 3 we show four sets of measurements on four tubes showing the half of the separation between the two press surfaces, b, as a function of the mass read on the scale, m_e. Every tube was made from nominally identical foils (denoted set 1) from the same package with the thickness 190 $\pm$ 7 μm. We have rolled the foils along their longer side so that $h = 210$ mm. We see that the dependence $b \propto m_e^{-1/2}$ is obeyed by the data for sufficiently pressed foils, $b < 0.7\langle b_0 \rangle$. From the numerical analysis we conclude that an easy, yet very accurate way to obtain the bending rigidity of the foils is to fit the experimental data to the

$$b = \sqrt{\frac{0.912\kappa\pi h}{2m_e g}} \tag{7}$$

dependence in the region $b < 0.7b_0$.

In addition to this, we investigate experimentally the predicted universality of the system by studying different springs. To this end, we have constructed two tubes from

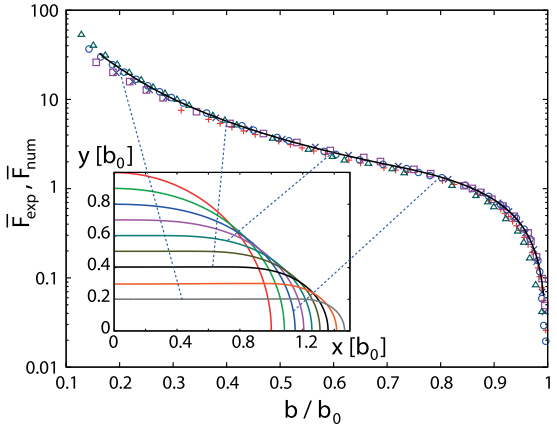

FIG. 4. (Color online) Scaled forces as specified by Eqs. (9) (line) and (8) (symbols). Circles and crosses correspond to the two sheets from set 1 rolled along the longer and shorter sides, respectively. Triangles and squares correspond to the two sheets from set 2 rolled along the longer and shorter sides, respectively. Pluses correspond to a measurement on a sheet from set 3 rolled along its longer side. The solid line shows the numerical results. The inset shows the calculated profiles of the spring for different pressing forces.

set 1 foils by rolling them along their length and width. We have tested two additional sets of sheets. For set 2 foils we used binding covers (A4 format) of smaller thickness (146 $\pm$ 8 μm). For set 3 we used A4 foils of thickness 412 $\pm$ 4 μm. For all measurements, we scaled the mass readings to produce the adimensional experimental force $\bar{F}_{\rm exp}$ as

$$\bar{F}_{\rm exp} = \frac{2m_e g b_0^2}{\pi\kappa h}. \tag{8}$$

The scale of force can be derived from the scale of energy $\pi\kappa h/b_0$ simply by dividing it by the scale of length, b_0 in our case. The quantity in Eq. (8) can be compared directly to its counterpart obtained from the numerical analysis,

$$\bar{F}_{\rm num} = -\frac{d\bar{E}_{\rm el}}{d(b/b_0)}. \tag{9}$$

Note that the factor of 2 in Eq. (8) arises from the fact that deformation of the tube where b changes by Δb requires applying the force of $m_e g$ on a distance of $2\Delta b$; the same factor of 2 is present in Eq. (2). The comparison of the scaled experimental readings with the numerical results is shown in Fig. 4. One can see that the scaling predicted by the numerical results is evident in the experimental data through an interval

TABLE I. Properties of the sheets used in experiments shown in Fig. 4 and bulk Young moduli of the sheets E calculated assuming a Poisson ratio of $\nu = 0.3$.

Sheet	h (cm)	d (μm)	κ (mJ)	E (GPa)
set 1	29.7	190	1.58	2.52
set 1	21.0	190	1.59	2.53
set 2	29.7	146	0.87	3.05
set 2	21.0	146	0.71	2.48
set 3	21.0	412	13.2	2.06

of almost four orders of magnitude of the force (in both the small- and large-deformation regimes). In the inset of Fig. 4 we show the profiles obtained by the numerical method (due to symmetry, it is sufficient to show only quarters of the profiles) corresponding to different parts of the universal curve.

A summary of the bending rigidities obtained for the sheets shown in Fig. 4 is shown in Table I. The fifth column of data contains the bulk Young modulus E of the sheets obtained from Eq. (1) using a value of κ determined experimentally and a Poisson ratio of $\nu = 0.3$ that is typical for most materials. The bulk Young moduli are indeed in the range expected for polymeric materials such as nylon ($E \sim 2$–4 GPa).

In conclusion, we have investigated theoretically and experimentally small and large radial deformations of a tube made from a sheet of thin elastic material. We have obtained a (scaled) universal response curve of the system. The numerical solution of the problem was compared with two simple *Ansatz* trial functions that represent the linear (ellipse) and nonlinear (stadium) responses of the tube. The stadium profile of the pressed cylinder is found to be an excellent approximation when compared to our numerical simulations and it predicts a correct analytical dependence of the energy and the reaction force of the deformed tube.

Note added in proof. We would like to mention a recently published paper related to our work by Kashcheyevs [18].

We thank Hrvoje Mesić for helping to design the experimental setup and suggesting the use of a kitchen scale below the press to measure force, Tomislav Vuletić for designing the setup that we actually used, and the Croatian Ministry of Science for financial support (Grants No. 035-0352828-2837 and No. 119-0000000-1015).

[1] L. Boué, M. Adda Bedia, A. Boudaoud, D. Cassani, Y. Couder, A. Eddi, and M. Trejo, Phys. Rev. Lett. **97**, 166104 (2006).
[2] M. Hasegawa and K. Nishidate, Phys. Rev. B **74**, 115401 (2006).
[3] A. Šiber and R. Podgornik, Phys. Rev. E **79**, 011919 (2009).
[4] P. K. Purohit, J. Kondev, and R. Phillips, Proc. Natl. Acad. Sci. USA **100**, 3173 (2003); A. Šiber, M. Dragar, V. A. Parsegian, and R. Podgornik, Eur. Phys. J. E **26**, 317 (2008).
[5] M. A. Glaser, G. M. Grason, R. D. Kamien, A. Košmrlj, C. D. Santangelo, and P. Ziherl, Europhys. Lett. **78**, 46004 (2007).
[6] J. Tersoff and R. S. Ruoff, Phys. Rev. Lett. **73**, 676 (1994); S.-P. Chan, W.-L. Yim, X. G. Gong, and Z.- F. Liu, Phys. Rev. B **68**, 075404 (2003).
[7] A. Hočevar and P. Ziherl, Phys. Rev. E **80**, 011904 (2009).
[8] I. Palaci, S. Fedrigo, H. Brune, C. Klinke, M. Chen, and E. Riedo, Phys. Rev. Lett. **94**, 175502 (2005).
[9] W. C. Young and R. G. Budynas, *Roak's Formulas for Stress and Strain*, 7th ed. (McGraw-Hill, New York, 2002).
[10] J. Tersoff, Phys. Rev. B **46**, 15546 (1992).
[11] A. Šiber, Nanotechnology **17**, 3598 (2006); **18**, 375705 (2007).
[12] U. Seifert, Adv. Phys. **46**, 13 (1997); W. Helfrich, Z. Naturforsch. C **28**, 693 (1973).
[13] J. Lidmar, L. Mirny, and D. R. Nelson, Phys. Rev. E **68**, 051910 (2003).
[14] A. Šiber, Phys. Rev. E **73**, 061915 (2006).
[15] P. J. de Pablo, I. A. T. Schaap, F. C. MacKintosh, and C. F. Schmidt, Phys. Rev. Lett. **91**, 098101 (2003).
[16] R. A. Arciniega, C. M. Wang, and J. N. Reddy, in *Shell Structures: Theory and Applications*, edited by I. Kreja and W. Pietraszkiewicz (CRC, Leiden, 2010), Vol. 2, p. 11; A. Muc, *ibid.*, p. 87.
[17] Stephen P. Timoshenko and James P. Gere, *Theory of Elastic Stability*, 2nd ed. (McGraw-Hill International, New York, 1963).
[18] V. Kashcheyevs, Am. J. Phys. **79**, 657 (2011).